

Published in final edited form as:

*J Chem Neuroanat.* 2013 September ; 52: 25–35. doi:10.1016/j.jchemneu.2013.04.004.

## A Subset of Presympathetic-Premotor Neurons within the Centrally Projecting Edinger-Westphal Nucleus Expresses Urocortin-1

Najmul S. Shah<sup>1,†,‡</sup>, Phyllis C. Pugh<sup>1,‡</sup>, Hyungwoo Nam<sup>1</sup>, Devin T. Rosenthal<sup>2</sup>, Diane van Wijk<sup>3</sup>, Balazs Gaszner<sup>4</sup>, Tamas Kozicz<sup>3</sup>, and Ilan A. Kerman<sup>1,\*</sup>

<sup>1</sup>Department of Psychiatry and Behavioral Neurobiology, University of Alabama at Birmingham, Birmingham, AL, USA <sup>2</sup>Boston Biomedical, Boston, MA, USA <sup>3</sup>Radboud University Nijmegen Medical Centre, Nijmegen, Netherlands <sup>4</sup>Department of Anatomy, Pécs University, Pécs, Hungary

### Abstract

Numerous motivated behaviors require simultaneous activation of somatomotor and autonomic functions. We have previously characterized the organization of brain circuits that may mediate this integration. Presympathetic premotor neurons (PSPMN) that are part of such circuits are distributed across multiple brain regions, which mediate stress-elicited behavioral and physiological responses, including the Edinger-Westphal nucleus (EW). Based on its connectivity and function, EW has recently been re-classified into a preganglionic (EWpg) and a centrally-projecting (EWcp) population. Neurons within EWcp are the major source of urocortin 1 (Ucn-1), an analogue of the corticotropin-releasing factor that binds the CRFR1 and CRFR2 receptors and has been implicated in mediating homeostatic responses to stress. We hypothesized that a subset of EWcp PSPMN expresses Ucn-1. Utilizing dual-label immunofluorescence, we initially mapped the distribution of Ucn-1 and cholinergic neurons within EW in colchicine pre-treated rats. Based on this labeling we divided EWcp into three neuroanatomical levels. To examine connections of EWcp neurons to the gastrocnemius muscle and the adrenal gland, we next employed trans-synaptic tract-tracing in a second group of rats, utilizing two pseudorabies virus (PRV) recombinants that express unique reporter proteins. Using multi-label immunofluorescent staining, we identified the presence of Ucn-1-positive PSPMN, dually labeled with PRV and present throughout the entire extent of EWcp and intermingled with Ucn-1 neurons infected with one or neither of the viral recombinants. Compared to rats pretreated with colchicine, we observed significantly fewer Ucn-1 neurons in animals that received PRV injections. Post-hoc analyses revealed significantly fewer Ucn-1 neurons at the rostral level as compared to the caudal and middle levels, while the total number of PRV-infected neurons was greatest at the middle level of EWcp. These data suggest functional and anatomic heterogeneity within EWcp; this organization may coordinate various aspects of stress-elicited and emotionally-salient behaviors.

© 2013 Elsevier B.V. All rights reserved.

\*Corresponding Author: Sparks Center 743, 1720 7<sup>th</sup> Avenue South, Birmingham, AL 35294, kerman@uab.edu, (205)975-0310 – voice, (205)975-4879- fax.

‡These authors contributed equally to this work.

†present address: College of Human Medicine, Michigan State University, East Lansing, MI, USA

**Publisher's Disclaimer:** This is a PDF file of an unedited manuscript that has been accepted for publication. As a service to our customers we are providing this early version of the manuscript. The manuscript will undergo copyediting, typesetting, and review of the resulting proof before it is published in its final citable form. Please note that during the production process errors may be discovered which could affect the content, and all legal disclaimers that apply to the journal pertain.

## Keywords

pseudorabies virus; stress; rat; muscle; adrenal gland

---

## 1. Introduction

Numerous stress-elicited behaviors require concomitant activation of somatic motor and autonomic outflows (Futuro-Neto and Coote, 1982a, b; Hilton, 1982; Jordan, 1990; Mancia and Zanchetti, 1981; Morrison, 2004; Waldrop *et al.*, 1996). Such coordination is likely mediated by multiple parallel descending circuits that link stress-regulatory brain regions with those that integrate physiological functions. In our previous work, we used retrograde trans-synaptic tract-tracing with pseudorabies virus (PRV) to identify neurons in the brain sending descending projections with poly-synaptic collaterals to skeletal muscle and the adrenal gland [see (Kerman, 2008) for review]. Termed presympathetic premotor neurons (PSPMN), these cells were located within discrete sites throughout the brain. At early survival times, PSPMNs were found predominantly within the ventromedial medulla, the ventrolateral periaqueductal gray, the paraventricular nucleus of the hypothalamus (PVN), and the lateral hypothalamus, suggesting that these regions contain PSPMNs with direct projections to the spinal cord (Kerman *et al.*, 2003; Kerman *et al.*, 2006b). At longer survival times these primary brain regions increased their numbers of dually-infected neurons, while such neurons also appeared within additional regions of the brainstem, hypothalamus, and cortex (Kerman *et al.*, 2006b).

The organization of this circuitry suggests that the PSPMNs may play a role in mediating stress-elicited adaptive behaviors. Spatially segregated populations of these neurons in the lateral hypothalamus contain either orexins or melanin-concentrating hormone (MCH). In the paraventricular nucleus of the hypothalamus (PVN) subsets of PSPMNs express either oxytocin (OT) or arginine vasopressin (AVP) (Kerman *et al.*, 2007; Kerman *et al.*, 2006b). Behavioral and physiological studies have documented the important roles of these transmitter systems in mediating stress-elicited adaptive responses. Peri-fornical orexinergic neurons within the lateral hypothalamus mediate tachycardia and contractions of the large muscle groups associated with the fight-or-flight response (Kayaba *et al.*, 2003; Samson *et al.*, 2007), while MCH neurotransmission mediates anxiety-related motor and cardiovascular responses (Borowsky *et al.*, 2002; Marsh *et al.*, 2002; Messina and Overton, 2007). Similarly, neuroactive peptide systems of the PVN, including AVP and OT, have long been implicated in mediating a variety of emotionally- and stress- elicited endocrine, autonomic, and motor responses (Bao *et al.*, 2008; Murgatroyd *et al.*, 2004; Rinaman *et al.*, 1995; Veenema and Neumann, 2007).

In addition to these nuclei in the brainstem and the hypothalamus, we also observed PSPMNs with the Edinger-Westphal nucleus (EW) of the midbrain (Kerman *et al.*, 2006a). This nucleus has long been recognized as an important regulator of the autonomic outflow to the eye (Westphal, 1887). However, more recent studies have identified EW as source of urocortin 1 (Ucn-1) in the brain (Bittencourt *et al.*, 1999; Kozicz *et al.*, 2011a; Kozicz *et al.*, 2011b; Kozicz *et al.*, 1998; Vaughan *et al.*, 1995). A neuroactive peptide, Ucn-1 is related to the corticotropin releasing factor (CRF) and exhibits strong affinity for the CRF1 and CRF2 receptors (Vaughan *et al.*, 1995). It is synthesized exclusively within neurons of the centrally-projecting subdivision of EW (EWcp), spatially segregated from the cholinergic neurons that innervate the ciliary ganglion located in the preganglionic portion of EW (EWpg) (Cavani *et al.*, 2003; Kozicz *et al.*, 2011a; Ryabinin *et al.*, 2005; Ryabinin *et al.*, 2012; Weninger *et al.*, 1999). Behavioral and pharmacologic studies have demonstrated that Ucn-1 neurons are activated by acute stressors, including restraint and pain (Gaszner *et al.*,

2004). In addition, systemic administration of Ucn-1 precipitates anxiety-like behaviors with strong motor and autonomic components (Moreau *et al.*, 1997; Skelton *et al.*, 2000).

Taken together these observations suggest that descending PSPMN within the EWcp contain Ucn-1 and may contribute to stress-elicited behavioral responses that require integration of somatic motor and sympathetic responses. To test this hypothesis, we first examined the distribution of Ucn-1 neurons of the EW relative to its cholinergic cells in cholchicine-pretreated rats. In a separate cohort of animals, we then combined retrograde trans-synaptic tract-tracing with PRV recombinants with multi-label immunofluorescence to identify Ucn-1-positive PSPMNs.

## 2. Methods

All of the procedures regarding animal use in this study were consistent with the National Academy of Sciences *Guide for the Care and Use of Laboratory Animals* (1996, National Academy of Sciences) and approved by the local Institutional Animal Use and Care Committee.

### 2.1 Animal Use

Distribution of Ucn-1-containing and cholinergic neurons in the EW was mapped in male Sprague-Dawley rats (n=3), which were bred locally at the Central Animal Lab at Pécs University Medical Faculty, and were injected with colchicine (50 mg icv dissolved in 0.02 ml of aCSF) to increase Ucn-1 levels in the soma. Following 72-hour survival the animals were deeply anesthetized with nembutal (100 mg/kg body weight i.p.; Sanofi-Synthélabo, Budapest, Hungary), and transcardially perfused with 4% paraformaldehyde fixative. All animal handling was conducted in accordance with the Medical Faculty Advisory Committee for Animal Resources of Pécs University, Medical Faculty, Pécs, Hungary based on the Law of 1998, XXVIII, for Animal Care and Use in Hungary.

Trans-synaptic tract-tracing was performed in male Sprague-Dawley rats (n = 8; Charles River Laboratories, Wilmington, MA) (see Table 1). We previously observed a negative correlation between weight and the rate of motoneuron infection, with an optimal weight of approximately 200 g (Kerman *et al.*, 2003). In light of this finding, we used rats that weighed between 163 and 254 g, with an average of  $199 \pm 11$  g [ mean  $\pm$  SEM; weighed at the time of sympathectomy (see below)]. Animals were anesthetized with 5% isoflurane vaporized in 1-1.5 L/min of O<sub>2</sub> and were maintained with a 1.5-2.5% concentration. Surgical plane of anesthesia was achieved such that there was no spontaneous movement and no withdrawal responses to tail and/or foot pinch. Prior to PRV injections, we removed sympathetic innervation to the hindlimb musculature. Surgical sympathectomy was performed as previously described (Kerman *et al.*, 2006a; Kerman *et al.*, 2003). Briefly, a ventral laparotomy was performed and a segment of the lumbar sympathetic nerve from the level of the renal artery to the aortic bifurcation was extirpated. Neural plexuses along the abdominal aorta were stripped off under microscopic observation using fine forceps, and the aorta was swabbed with a 10% phenol solution. We previously validated the effectiveness of this sympathectomy method by the lack of PRV infection within the intermediolateral cell column at short survival times (Kerman *et al.*, 2003). Following a 2-10 day recovery period the animals were injected with 30  $\mu$ l of PRV-152 into the left gastrocnemius muscle and 2-4  $\mu$ l of PRV-BaBlu into the left adrenal gland as previously described (Kerman *et al.*, 2003). To achieve temporal matching of the infection from the two organs, injections into the muscle and the adrenal gland were separated by 24 hours (Kerman *et al.*, 2003). After a survival time of 120-144 hours post-PRV-152 injections, the rats were deeply anesthetized with sodium pentobarbital (150 mg/kg) and were transcardially perfused with 100-150 mL

of physiological saline (0.9% NaCl) followed by 400-500 mL of paraformaldehyde l-lysine sodium metaperiodate (PLP) fixative (McLean and Nakane 1974).

We used recombinant strains of PRV, which express unique reporter proteins, with PRV-152 expressing enhanced green fluorescent protein (EGFP) and PRV-BaBlu transcribing  $\beta$ -galactosidase (Billig *et al.*, 2000). Both of these strains were derived from an attenuated strain – PRV-Bartha that is not infectious to humans but has been demonstrated to have the capability of simultaneous neuronal co-infection in rats (Billig *et al.*, 2000; Standish *et al.*, 1995). Viral stocks were harvested from pig kidney cell cultures at a titer of  $10^8$ - $10^9$  pfu/mL, aliquoted into 50  $\mu$ L volumes, and stored at  $-80^\circ\text{C}$  until the time of inoculations at which time they were rapidly thawed in a  $37^\circ\text{C}$  water bath. PRV injections were performed as previously described (Kerman *et al.*, 2003; Kerman *et al.*, 2006b). Briefly, the gastrocnemius muscle was injected using a 10  $\mu$ L glass syringe (Hamilton Company, Reno, NV), which was used to deliver 1  $\mu$ L volumes of PRV-152 (totaling 30  $\mu$ L) throughout the lateral head of the gastrocnemius muscle. PRV-BaBlu was similarly injected using a Hamilton syringe and a glass pipette, attached to the tip with wax. A total of 2-4  $\mu$ L of PRV-BaBlu was injected into the ipsilateral adrenal gland.

## 2.2 Tissue Processing

Brains from colchicine injected animals were processed for Ucn-1 and choline acetyltransferase (ChAT) double immunofluorescence. Following perfusions, brains were extracted, post-fixed overnight, and cryoprotected in 20% sucrose. Tissue was sectioned coronally on a freezing microtome at a thickness of 25  $\mu$ m and stored at  $-20^\circ\text{C}$  in cryoprotectant [30% sucrose, 30% ethylene glycol, 1% polyvinyl-pyrrolidone (PVP-40)] until immunohistochemical processing. Free-floating tissue sections were reacted with 1:1,000 rabbit anti-Ucn-1 antibody (generous gift of Dr. Wylie Vale, Salk Institute for Biological Studies) and 1:5,000 goat anti-ChAT antibody (# AB144P from Millipore, <http://www.millipore.com/>). Cy2-conjugated anti-goat IgG (1:80) and Cy3-conjugated anti-rabbit IgG (1:100) (Jackson ImmunoResearch Labs, West Grove, PA, USA) were used to visualize Ucn-1- and ChAT- positive neurons, respectively. Sections were mounted onto glass slides and coverslipped with an anti-fade medium (Vectashield, Vector Labs, Burlingame, CA, USA).

Brains from PRV-injected animals were processed for triple immunofluorescent detection of: EGFP,  $\beta$ -galactosidase, and Ucn-1. Following perfusions, brains were extracted, post-fixed overnight, and immersed in 20-30% sucrose overnight. Brains were sectioned coronally on a freezing microtome at a thickness of 40  $\mu$ m and stored at  $-20^\circ\text{C}$  in cryoprotectant until immunohistochemical processing. Free-floating brain sections were rinsed with 0.1 M phosphate buffer (PB; pH 7.4) several times at room temperature and then incubated for 1 hour in 1% normal goat serum (NGS), 1% bovine serum albumin (BSA), and 0.3% Triton X-100 (TX-100) in 0.1 M PB. Sections were then reacted with a cocktail of primary antibodies: chicken anti-GFP IgY (Abcam, Cambridge, MA, product 13970) at 1:2,000, mouse anti- $\beta$ -galactosidase IgG (Sigma, St. Louis, MO, product G4644) at 1:1,000, and rabbit anti-urocortin 1 (Ucn-1; obtained from Dr. Wylie Vale) at 1:500 in a solution that contained 1% NGS, 1% BSA, 0.3% TX-100 and 1 mg/ml of heparin. Following a 48-hour incubation at  $4^\circ\text{C}$ , the tissue was rinsed with 0.1 M PB and reacted with a secondary antibody cocktail of: Cy3-conjugated donkey anti-mouse IgG (1:200; Jackson ImmunoResearch), AlexaFluor488-conjugated goat anti-chicken IgG (1:200; Life Technologies, <http://www.lifetechnologies.com>), and AlexaFluor 647-conjugated goat anti-rabbit IgG (1:200; Life Technologies), dissolved in 1% NGS, 1% BSA, and 0.3% TX-100 in 0.1 M PB. Following processing, tissue sections were mounted on glass slides and coverslipped with Aqua Poly/Mount (Polysciences, Inc., <http://www.polysciences.com/>).

## 2.3 Antibody Characterization

The chicken anti-GFP antibody was raised against the recombinant full-length protein. This antibody yields a single band on Western blot and detects GFP in transgenic mice expressing GFP in lamina II of the spinal cord (manufacturer's technical information). We previously did not detect staining with this antibody in brain sections from rats not infected with PRV-152 (Kerman *et al.*, 2003). Mouse anti- $\beta$ -galactosidase antibody was developed in mouse peritoneal cavities using  $\beta$ -galactosidase purified from *E. coli* as the immunogen (manufacturer's technical information). Using Western blot, this antibody was shown to be specific for  $\beta$ -gal in its native form (116 kD), and it reacts only with  $\beta$ -gal from *E. coli* (manufacturer's technical information). Specificity of this antibody in immunofluorescent experiments has been previously documented (Kerman *et al.*, 2003). The anti-Ucn-1 antiserum (from Dr. Wylie Vale, PBL No. 5779) was generated in rabbit against Ucn-1 coupled to human  $\gamma$ -globulin via glutaraldehyde as the immunogen, and its specificity previously documented with radioimmunoassay (Turnbull *et al.*, 1999). Specificity of the anti-ChAT antibody was determined by preabsorption with 1  $\mu$ g of the synthetic immunizing peptide, which completely abolished immunostaining in the rat EWcp (data not shown).

## 2.4 Tissue Analysis

Immunofluorescently-labeled tissue was examined using Olympus microscopes: BX61 and Olympus FluoView 1000 laser scanning confocal microscope (<http://www.olympusamerica.com/>). BX61 was equipped with a motorized stage (96S100-LE; Ludl Electronic Products, <http://www.ludl.com/>), fluorophore-specific fluorescent filter sets (excitation and emission spectra: AlexaFluor 488/FITC – 482/35, 536/40; Cy3/TRITC – 531/40, 593/40; AlexaFluor 647 – 628/40, 692/40), and a cooled mono CCD camera (Orca R2; Hamamatsu, <http://hamamatsucameras.com/>). Ucn-1/ChAT double-labeled material was examined at 75  $\mu$ m intervals, while PRV-infected brains were examined at 240  $\mu$ m intervals. Stitched images of EW were acquired using the driven stage with excitation/emission settings appropriate for each fluorophore and then pseudocolored. Overlaid TIFFs were imported into NeuroLucida software (MBF Bioscience; <http://www.mbfioscience.com/>) for mapping of the different classes of immunofluorescently-labeled neurons. Figures were prepared using Adobe Photoshop CS5 (<http://www.adobe.com/>) that was used to optimize brightness and contrast were optimized for presentation purposes.

## 2.5 Statistical Analyses

Data were analyzed with Prism 6.0 (GraphPad Software, San Diego, CA) using two-way ANOVAs. Anatomical level and cell type were fixed factors and number of cells per section was the dependent variable; post-hoc comparisons were evaluated with an appropriate test based on the distribution of values. Significance was set as  $p < 0.05$ .

## 3. Results

### 3.1 Distribution of Ucn-1 and Cholinergic neurons

Ucn-1-positive neurons formed a midline column that stretched rostrally for greater than 1 mm starting at the level of the third nerve nucleus (3N; Fig. 1). At their caudal extent, these cells formed a diamond-like shape located dorsally and medially relative to the cholinergic neurons of 3N and the EWpg (Fig 1A-D). More rostrally and past the major population of the cholinergic neurons, at the level of the rostral tip of the red nucleus, the Ucn-1 neurons formed two populations. The first was a column of cells extending dorsoventrally along the midline, and the second population was laterally displaced neurons that formed a diagonal band extending ventrally and laterally from the midline (Fig. 1E-J). At their most rostral extent, at the level of the posterior commissure, Ucn-1 neurons were very loosely distributed

and did not form a distinct shape or nucleus (Fig. 1K-O). Rostrally, Ucn-1<sup>+</sup> neurons tend to be pyramidal, with a dorsoventrally oriented dendritic tree; this is also true for the middle group. The caudal group of Ucn-1<sup>+</sup> neurons are somewhat larger and more multipolar in nature. In comparison, ChAT<sup>+</sup> neurons within 3N are large and those within the EWpg are small and oriented at the midline. Without colchicine pre-treatment, e.g., rats injected with PRV, Ucn-1 levels were lower, but the location of the neurons remained the same (Table 2).

Based on these observations, we divided EWcp into: caudal (Fig. 2A), middle (Fig. 2B), and rostral (Fig. 2C) subdivisions. Most of the cholinergic and Ucn-1 neurons were spatially segregated; however, some of the cholinergic neurons were also located along the midline and were intermingled among the Ucn-1 neurons. A few of these cells were double-labeled with ChAT and Ucn-1 (see Fig. 1B) and most appeared to be located along the midline at the middle level of the EWcp (Fig. 2B). Further analyses suggest that at the middle and rostral levels, approximately 40% of the ChAT<sup>+</sup> neurons also contain Ucn-1 ( $45.2 \pm 10.6\%$ ,  $n = 13$  sections and  $41.7 \pm 17.7\%$ ,  $n = 9$  sections, respectively, Fig. 3B). This co-localization is not simply due to the differences in numbers of Ucn-1<sup>+</sup> cells, as the number of co-labeled cells does not co-vary with the number of Ucn-1<sup>+</sup> cells (linear analysis, slope =  $0.01532 \pm 0.03182$ ,  $R^2 = 0.1883$ , Fig. 3C). In rats injected with PRV, Ucn-1-positive neurons were similarly distributed, but they appeared fewer in number.

Two-way ANOVA revealed significant interaction between cell type and neuroanatomical level in their impact on neuronal density per section ( $p < 0.01$ ; Table 2). Main effect analyses demonstrated significantly greater numbers of Ucn-1 neurons in the colchicine-treated rats ( $p < 0.01$ ). Post-hoc analyses revealed nearly twice as many Ucn-1 neurons in the colchicine-treated animals at the caudal ( $p < 0.01$ ) and middle ( $p < 0.01$ ) levels of EWcp (Table 2). At the rostral level there was a significant decrease in the numbers of Ucn-1 neurons in the colchicine-treated animals as compared to the caudal ( $p < 0.01$ ) and middle ( $p < 0.005$ ) levels. No differences in the numbers of Ucn-1 neurons between PRV- and colchicine-injected animals were detected at the rostral level ( $p > 0.5$ ).

### 3.2 Co-localization of Ucn-1 and PRV

Based on their survival times and the pattern of labeling in EWcp, animals were assigned to short, intermediate, or long survival groups (Table 1). Rats in the short survival group ( $n = 2$ ) survived 96 or 97 hours following PRV-BaBlu injections and 120 or 122 hours following PRV-152. In the intermediate survival group the animals ( $n = 4$ ) survived 108 or 112 hours (PRV-BaBlu) and 132 or 136 hours (PRV-152), or 119 hours (PRV-BaBlu) and 143 hours (PRV-152). In the long survival group the rats survived 111 or 120 hours (PRV-BaBlu) and 144 hours (PRV-152).

In line with our previous observations, we detected considerable number of PRV-infected neurons within EWcp throughout its rostro-caudal extent (Fig. 4). Examination of this material at higher magnification revealed a number of single- and double- infected neurons with EWcp that also expressed Ucn-1 (Fig. 5). Neurons that expressed Ucn-1 and were infected with either or both PRV recombinants were detected at the earliest survival time, while the numbers of double-infected neurons increased with longer survival times as did their co-localization with Ucn-1 (Fig. 6). Distribution of these neurons is quantified in both Fig. 7 and Table 3.

## 4. Discussion

In the current study we utilized dual-label immunofluorescence for Ucn-1 and ChAT to demonstrate rostro-caudal differences in the appearance and cell density of EWcp. Our data demonstrate distinct patterns of distribution of Ucn-1-containing neurons at the caudal,

middle, and rostral levels of EWcp, with its rostral-most extent containing significantly fewer neurons. We then utilized retrograde trans-synaptic tract-tracing with PRV recombinants to demonstrate the presence of neurons that send poly-synaptic projections to the gastrocnemius muscle and/or the adrenal gland within EWcp. Significantly greater number of PRV-infected neurons was located at the middle rostro-caudal level. We detected neurons infected with one or both of the PRV recombinants and expressing Ucn-1 at the earliest point of PRV infection within the EWcp. The numbers of co-localized neurons appeared to increase with longer survival times. Together these observations point to connectional, and thus possibly functional, heterogeneity within EWcp.

#### 4.1 Methodological Considerations

Similar to the other neuroactive peptides, Ucn-1 is synthesized in the cell body and rapidly transported to the nerve terminal, diminishing its immunofluorescent detection at the soma. To circumvent this issue, we inhibited axonal transport in a subset of animals via pre-treatment with colchicine in order to maximize the number of detectable Ucn-1-expressing neuronal somata in EWcp. Comparison of our cell counts between colchicine- and PRV-injected animals indicates that we detect significantly greater number of Ucn-1 neurons within the colchicine group. PRV-induced inhibition of native peptide synthesis in the host neuron likely contributed to this difference (Card, 2001; Kim *et al.*, 1999). Further, because colchicine treatment is also inherently stressful, it may also induce an increase in Ucn-1 expression neurons and contribute to this difference (Bittencourt *et al.*, 1999). Lastly, while both studies were conducted in the Sprague Dawley rat strain, the actual animals came from two different breeding populations. Given the previous demonstration that two different strains of mice (C57BL/6J and DBA/2J) had differing numbers of the Ucn-1<sup>+</sup> neurons in the EW, it is possible that a slight variation in strain genetics could also have contributed to this variability (Weitemier *et al.*, 2005). Therefore, our cell counts may not represent baseline numbers of Ucn-1 neurons in EWcp. Future studies employing non-stressful techniques that retain high levels of sensitivity will be required to address this issue.

In our tract-tracing studies we detected PRV-infected neurons that expressed Ucn-1 across multiple survival time points, beginning with the shortest survival time point at which PRV infected neurons are detected in the brain (Kerman *et al.*, 2003). While the numbers of PRV and Ucn-1 co-localized neurons increased with survival times, their overall fraction remained relatively low (less than 20% over all levels). However, given the difficulty of immunofluorescent detection of Ucn-1 in non-colchicine-treated rats along with PRV-mediated knockdown in host cell peptide expression (Card, 2001), these numbers likely represent an underestimate of the Ucn-1 neurons with descending poly-synaptic projections to the gastrocnemius muscle and/or the adrenal gland.

#### 4.2 Rostro-Caudal Differences

Our observations suggest rostro-caudal heterogeneity in the function and connectivity of EWcp. These include differences in the distribution of Ucn-1 neurons, their density, and their relationship to the nearby cholinergic neurons across the rostro-caudal extent. Caudally the Ucn-1 cells form a compact rhomboid-like structure that is dorsomedial to the nearby cholinergic neurons. At the middle level these cells form two columns: 1) a dorsoventral along the midline and 2) a ventrolaterally-displaced one. Rostrally these cells become loosely scattered. We also observed a small number of Ucn-1/ChAT double-labeled neurons, which appeared most numerous along the midline at the middle rostro-caudal level. However, their low number precluded us from statistically testing this observation. Emerging studies have implicated Ucn-1 in diverse functions, including alcohol intake, anxiety-like behavior, and stress-induced behavioral responses (Kozicz *et al.*, 2011b; Ryabinin *et al.*, 2012). The differences in the numbers of Ucn-1 neurons between colchicine-

and PRV- injected rats are significant at the caudal and middle, but not rostral, levels. Our tract-tracing studies have also revealed a significantly greater number of neurons with poly-synaptic projections to the gastrocnemius muscle and/or the adrenal gland at the middle level as compared to the caudal and rostral levels. Taken together with our observations, it seems feasible that these different functions may be mediated by spatially-segregated Ucn-1 neurons in the EWcp. Consistent with this, a previous report has documented significant differences in the numbers of Ucn-1 neurons in rats with inborn differences alcohol consumption. These differences in cell numbers also correlated with differences in Ucn-1 fiber density within the lateral septum, suggesting that the Ucn-1 neurons within EWcp that project to the lateral septum may mediate differences in alcohol consumption (Turek *et al.*, 2005). A second study showed similar differences between alcohol-preferring and Wistar male rats (Fonareva *et al.*, 2009). In the latter study, similar numbers of Ucn-1<sup>+</sup> neurons were seen at the rostral-most level, although they saw more Ucn-1<sup>+</sup> neurons at their middle (Bregma -5.41 to -6.20) and caudal (Bregma -6.21 to -7.00) levels (Fonareva *et al.*, 2009). Thus, our current data agree on multiple levels of Ucn-1 staining across the rostral-caudal extent of the EWcp. (Bao *et al.*, 2008) (Bao *et al.*, 2008) (Bao *et al.*, 2008) (Bao *et al.*, 2008) (Bao *et al.*, 2008)

### 4.3 Connectional Considerations

Previous studies have documented the presence of PRV-infected neurons in EWcp following injections of PRV into a variety of sympathetically-innervated organs, including the kidney, brown adipose tissue, and the spleen (Cano *et al.*, 2003; Cano *et al.*, 2001; Zhang *et al.*, 2011). We confirmed these observations and further extended them by demonstrating that the pre-sympathetic neurons are intermingled with PSPMNs in the EWcp and are observed at the earliest survival times at which appreciable infection with PRV is detected in the brain, suggesting their direct projections to the spinal cord. A fraction of these PRV-infected neurons also expressed Ucn-1, suggesting that a subset of Ucn-1 neurons in EWcp send descending projections to the spinal cord where they act to regulate the activation of sympathetic and somatomotor systems. These observations are in line with previous reports that utilized monosynaptic tract-tracing to demonstrate the presence of a direct projection from EW to the spinal cord along with those that reported the presence of Ucn-1 fibers in the spinal cord (Bittencourt *et al.*, 1999; Lakke, 1997). Ucn-1-positive fibers in the spinal cord are present within laminae VII and X, which contain sympathetic preganglionic neurons, along with lamina IX, which contains the alpha motoneuron pool of the ventral horn (Korosi *et al.*, 2007). These spinal regions also express CRFR2 receptors that are closely apposed to the Ucn-1 fibers, suggesting a mechanism by which PSPMNs within EWcp may regulate motor and sympathetic responses.

In addition to the descending projections to spinal cord, it is likely that higher order Ucn-1-containing PSPMNs are contained within the EWcp. Our finding of increasing numbers of such neurons with increasing survival times suggests that additional populations of neurons that do not send direct spinal projections exist within EWcp. Tract-tracing studies have demonstrated projections from EWcp to the dorsal raphe, the lateral septum, and the hypothalamus (Kozicz *et al.*, 2011a). In our earlier tract-tracing studies with PRV we observed labeling within the lateral subdivisions of the dorsal raphe and several hypothalamic subregions, including its paraventricular, lateral, and dorsomedial nuclei, at early survival times (Kerman, 2008). It is feasible that some of the Ucn-1 PSPMNs at the longer survival times project to these brainstem and/or hypothalamic regions.

### 4.4 Perspectives

Our data indicate neuroanatomical heterogeneity in the organization of EWcp. This includes rostro-caudal differences in the: 1) distribution of Ucn-1 neurons, 2) sensitivity of Ucn-1

neurons to colchicine, and 3) numbers of neurons with poly-synaptic projections to the adrenal gland and/or the gastrocnemius muscle. Given the important role of the CRF signaling in mediating stress-evoked behavioral and physiological responses along with its contribution to the etiology of depression and anxiety (Arborelius *et al.*, 1999; Ryabinin *et al.*, 2012), it is feasible that the Ucn-1-containing PSPMNs may play a role in stress-elicited motor and autonomic integration and that their dysfunction may contribute to the physical symptoms of mood disorders.

## Acknowledgments

This study was supported by NIH grant 5R00MH081927-04 (IAK) and the NARSAD Young Investigator Award awarded (IAK). The authors are grateful to Drs. Sarah Clinton, Mathieu Lesort, and S. J. Watson for their helpful comments and advice. NeuroLucida studies were made possible through the Neuroimaging Core at UAB (NS057098 and P30 HD038985). PRV stocks were provided by Dr. Lynn Enquist, Princeton University, Virus Center grant P40 OD010996.

## References

- Arborelius L, Owens MJ, Plotsky PM, Nemeroff CB. The role of corticotropin-releasing factor in depression and anxiety disorders. *J Endocrinol.* 1999; 160:1–12. [PubMed: 9854171]
- Bao AM, Meynen G, Swaab DF. The stress system in depression and neurodegeneration: focus on the human hypothalamus. *Brain Res Rev.* 2008; 57:531–553. [PubMed: 17524488]
- Billig I, Foris JM, Enquist LW, Card JP, Yates BJ. Definition of neuronal circuitry controlling the activity of phrenic and abdominal motoneurons in the ferret using recombinant strains of pseudorabies virus. *J Neurosci.* 2000; 20:7446–7454. [PubMed: 11007904]
- Bittencourt JC, Vaughan J, Arias C, Rissman RA, Vale WW, Sawchenko PE. Urocortin expression in rat brain: evidence against a pervasive relationship of urocortin-containing projections with targets bearing type 2 CRF receptors. *The Journal of comparative neurology.* 1999; 415:285–312. [PubMed: 10553117]
- Borowsky B, Durkin MM, Ogozalek K, Marzabadi MR, DeLeon J, Lagu B, Heurich R, Lichtblau H, Shaposhnik Z, Daniewska I, Blackburn TP, Branchek TA, Gerald C, Vaysse PJ, Forray C. Antidepressant, anxiolytic and anorectic effects of a melanin-concentrating hormone-1 receptor antagonist. *Nat Med.* 2002; 8:825–830. [PubMed: 12118247]
- Cano G, Passerin AM, Schiltz JC, Card JP, Morrison SF, Sved AF. Anatomical substrates for the central control of sympathetic outflow to interscapular adipose tissue during cold exposure. *The Journal of comparative neurology.* 2003; 460:303–326. [PubMed: 12692852]
- Cano G, Sved AF, Rinaman L, Rabin BS, Card JP. Characterization of the central nervous system innervation of the rat spleen using viral transneuronal tracing. *The Journal of comparative neurology.* 2001; 439:1–18. [PubMed: 11579378]
- Card JP. Pseudorabies virus neuroinvasiveness: a window into the functional organization of the brain. *Adv Virus Res.* 2001; 56:39–71. [PubMed: 11450308]
- Cavani JA, Reiner A, Cuthbertson SL, Bittencourt JC, Toledo CA. Evidence that urocortin is absent from neurons of the Edinger-Westphal nucleus in pigeons. *Braz J Med Biol Res.* 2003; 36:1695–1700. [PubMed: 14666254]
- Fonareva I, Spangler E, Cannella N, Sabino V, Cottone P, Ciccocioppo R, Zorrilla E, Ryabinin A. Increased perioculomotor urocortin 1 immunoreactivity in genetically selected alcohol preferring rats. *Alcoholism, clinical and experimental research.* 2009; 33:1956–1965.
- Futuro-Neto HA, Coote JH. Changes in sympathetic activity to heart and blood vessels during desynchronized sleep. *Brain Research.* 1982a; 252:259–268. [PubMed: 7150953]
- Futuro-Neto HA, Coote JH. Desynchronized sleep-like pattern of sympathetic activity elicited by electrical stimulation of sites in the brainstem. *Brain Research.* 1982b; 252:269–276. [PubMed: 7150954]
- Gaszner B, Csernus V, Kozicz T. Urocortinergic neurons respond in a differentiated manner to various acute stressors in the Edinger-Westphal nucleus in the rat. *The Journal of comparative neurology.* 2004; 480:170–179. [PubMed: 15514930]

- Hilton SM. The defence-arousal system and its relevance for circulatory and respiratory control. *Journal of Experimental Biology*. 1982; 100:159–174. [PubMed: 6816891]
- Jordan, D. Autonomic changes in affective behavior. In: Loewy, AD.; Spyer, KM., editors. *Central Regulation of Autonomic Functions*. Oxford University Press; New York: 1990. p. 349-366.
- Kayaba Y, Nakamura A, Kasuya Y, Ohuchi T, Yanagisawa M, Komuro I, Fukuda Y, Kuwaki T. Attenuated defense response and low basal blood pressure in orexin knockout mice. *Am J Physiol Regul Integr Comp Physiol*. 2003; 285:R581–593. [PubMed: 12750151]
- Kerman IA. Organization of brain somatomotor-sympathetic circuits. *Exp Brain Res*. 2008; 187:1–16. [PubMed: 18369609]
- Kerman IA, Akil H, Watson SJ. Rostral elements of sympatho-motor circuitry: a virally-mediated transsynaptic tracing study. *Journal of Neuroscience*. 2006a; 26:3423–3433. [PubMed: 16571749]
- Kerman IA, Bernard R, Rosenthal D, Beals J, Akil H, Watson SJ. Distinct populations of presympathetic-premotor neurons express orexin or melanin-concentrating hormone in the rat lateral hypothalamus. *The Journal of comparative neurology*. 2007; 505:586–601. [PubMed: 17924541]
- Kerman IA, Enquist LW, Watson SJ, Yates BJ. Brainstem substrates of sympatho-motor circuitry identified using trans-synaptic tracing with pseudorabies virus recombinants. *J Neurosci*. 2003; 23:4657–4666. [PubMed: 12805305]
- Kerman IA, Shabrang C, Taylor L, Akil H, Watson SJ. Relationship of presympathetic-premotor neurons to the serotonergic transmitter system in the rat brainstem. *The Journal of comparative neurology*. 2006b; 499:882–896. [PubMed: 17072838]
- Kim JS, Enquist LW, Card JP. Circuit-specific coinfection of neurons in the rat central nervous system with two pseudorabies virus recombinants. *J Virol*. 1999; 73:9521–9531. [PubMed: 10516061]
- Korosi A, Kozicz T, Richter J, Veening JG, Olivier B, Roubos EW. Corticotropin-releasing factor, urocortin 1, and their receptors in the mouse spinal cord. *The Journal of comparative neurology*. 2007; 502:973–989. [PubMed: 17444496]
- Kozicz T, Bittencourt JC, May PJ, Reiner A, Gamlin PD, Palkovits M, Horn AK, Toledo CA, Ryabinin AE. The Edinger-Westphal nucleus: a historical, structural, and functional perspective on a dichotomous terminology. *The Journal of comparative neurology*. 2011a; 519:1413–1434. [PubMed: 21452224]
- Kozicz T, Sterrenburg L, Xu L. Does midbrain urocortin 1 matter? A 15-year journey from stress (mal)adaptation to energy metabolism. *Stress*. 2011b; 14:376–383. [PubMed: 21438786]
- Kozicz T, Yanaihara H, Arimura A. Distribution of urocortin-like immunoreactivity in the central nervous system of the rat. *The Journal of comparative neurology*. 1998; 391:1–10. [PubMed: 9527535]
- Lakke EA. The projections to the spinal cord of the rat during development: a timetable of descent. *Adv Anat Embryol Cell Biol*. 1997; 135:I–XIV. 1–143. [PubMed: 9257458]
- Mancia, G.; Zanchetti, A. Hypothalamic control of autonomic functions. In: Morgane, PJ.; Panksepp, J., editors. *Behavioral studies of the hypothalamus*. Marcel Dekker; New York: 1981. p. 147-202.
- Marsh DJ, Weingarth DT, Novi DE, Chen HY, Trumbauer ME, Chen AS, Guan XM, Jiang MM, Feng Y, Camacho RE, Shen Z, Frazier EG, Yu H, Metzger JM, Kuca SJ, Shearman LP, Gopal-Truter S, MacNeil DJ, Strack AM, MacIntyre DE, Van der Ploeg LH, Qian S. Melanin-concentrating hormone 1 receptor-deficient mice are lean, hyperactive, and hyperphagic and have altered metabolism. *Proc Natl Acad Sci U S A*. 2002; 99:3240–3245. [PubMed: 11867747]
- Messina MM, Overton JM. Cardiovascular effects of melanin-concentrating hormone. *Regul Pept*. 2007; 139:23–30. [PubMed: 17045349]
- Moreau JL, Kilpatrick G, Jenck F. Urocortin, a novel neuropeptide with anxiogenic-like properties. *Neuroreport*. 1997; 8:1697–1701. [PubMed: 9189917]
- Morrison SF. Central pathways controlling brown adipose tissue thermogenesis. *News Physiol Sci*. 2004; 19:67–74. [PubMed: 15016906]
- Murgatroyd C, Wigger A, Frank E, Singewald N, Bunck M, Holsboer F, Landgraf R, Spengler D. Impaired repression at a vasopressin promoter polymorphism underlies overexpression of vasopressin in a rat model of trait anxiety. *J Neurosci*. 2004; 24:7762–7770. [PubMed: 15342744]

- Paxinos, G.; Watson, C. *The Rat Brain in Stereotaxic Coordinates*. 4. Academic Press; San Diego: 1998.
- Rinaman, L.; Sherman, TG.; Stricker, EM. Vasopressin and oxytocin in the central nervous system. In: Bloom, FE.; Kupfer, DJ., editors. *Psychopharmacology: The Fourth Generation of Progress*. Raven Press, Ltd.; New York: 1995. p. 531-542.
- Ryabinin A, Tsivkovskaia N, Ryabinin S. Urocortin 1-containing neurons in the human Edinger-Westphal nucleus. *Neuroscience*. 2005; 134:1317–1323. [PubMed: 16039794]
- Ryabinin AE, Tsoory MM, Kozicz T, Thiele TE, Neufeld-Cohen A, Chen A, Lowery-Gionta EG, Giardino WJ, Kaur S. Urocortins: CRF's siblings and their potential role in anxiety, depression and alcohol drinking behavior. *Alcohol*. 2012; 46:349–357. [PubMed: 22444954]
- Samson WK, Bagley SL, Ferguson AV, White MM. Hypocretin/orexin type 1 receptor in brain: role in cardiovascular control and the neuroendocrine response to immobilization stress. *Am J Physiol Regul Integr Comp Physiol*. 2007; 292:R382–387. [PubMed: 16902182]
- Skelton KH, Owens MJ, Nemeroff CB. The neurobiology of urocortin. *Regul Pept*. 2000; 93:85–92. [PubMed: 11033056]
- Standish A, Enquist LW, Escardo JA, Schwaber JS. Central neuronal circuit innervating the rat heart defined by transneuronal transport of pseudorabies virus. *J Neurosci*. 1995; 15:1998–2012. [PubMed: 7891147]
- Turek VF, Tsivkovskaia NO, Hyytia P, Harding S, Le AD, Ryabinin AE. Urocortin 1 expression in five pairs of rat lines selectively bred for differences in alcohol drinking. *Psychopharmacology (Berl)*. 2005; 181:511–517. [PubMed: 15983799]
- Turnbull AV, Vaughan J, Rivier JE, Vale WW, Rivier C. Urocortin is not a significant regulator of intermittent electrofootshock-induced adrenocorticotropin secretion in the intact male rat. *Endocrinology*. 1999; 140:71–78. [PubMed: 9886809]
- Vaughan J, Donaldson C, Bittencourt J, Perrin MH, Lewis K, Sutton S, Chan R, Turnbull AV, Lovejoy D, Rivier C, et al. Urocortin, a mammalian neuropeptide related to fish urotensin I and to corticotropin-releasing factor. *Nature*. 1995; 378:287–292. [PubMed: 7477349]
- Veenema AH, Neumann ID. Neurobiological mechanisms of aggression and stress coping: a comparative study in mouse and rat selection lines. *Brain Behav Evol*. 2007; 70:274–285. [PubMed: 17914259]
- Waldrop, TG.; Eldridge, FL.; Iwamoto, GA.; Mitchell, JH. Central neural control of respiration and circulation during exercise. In: Rowell, LB.; Shepherd, JT., editors. *Handbook of Physiology Section 12: Exercise: Regulation and Integration of Multiple Systems*. Oxford University Press; New York: 1996. p. 333-380.
- Weitemier A, Tsivkovskaia N, Ryabinin A. Urocortin 1 distribution in mouse brain is strain-dependent. *Neuroscience*. 2005; 132:729–740. [PubMed: 15837134]
- Weninger SC, Dunn AJ, Muglia LJ, Dikkes P, Miczek KA, Swiergiel AH, Berridge CW, Majzoub JA. Stress-induced behaviors require the corticotropin-releasing hormone (CRH) receptor, but not CRH. *Proc Natl Acad Sci U S A*. 1999; 96:8283–8288. [PubMed: 10393986]
- Westphal C. Über einen fall von chronischer progressiver Lähmung der Augenmuskeln (Ophthalmoplegia externa) nebst Beschreibung von Ganglienzellengruppen im Bereiche des Oculomotoriuskerns. *Arch Psychiat Nervenkr*. 1887; 98:846–871.
- Zhang Y, Kerman IA, Laque A, Nguyen P, Faouzi M, Louis GW, Jones JC, Rhodes C, Munzberg H. Leptin-receptor-expressing neurons in the dorsomedial hypothalamus and median preoptic area regulate sympathetic brown adipose tissue circuits. *J Neurosci*. 2011; 31:1873–1884. [PubMed: 21289197]

### Highlights

Urocortin-1 neurons were mapped within the Edinger-Westphal nucleus.

Urocortin-1-containing neurons within the Edinger-Westphal nucleus are distributed in a distinct rostral-caudal pattern.

Some of these urocortin-1 neurons also express cholinergic markers.

Neurons within the Edinger-Westphal nucleus send poly-synaptic projections to skeletal muscle and the adrenal gland.

Some of the Edinger-Westphal neurons that poly-synaptically project to the periphery express urocortin-1.

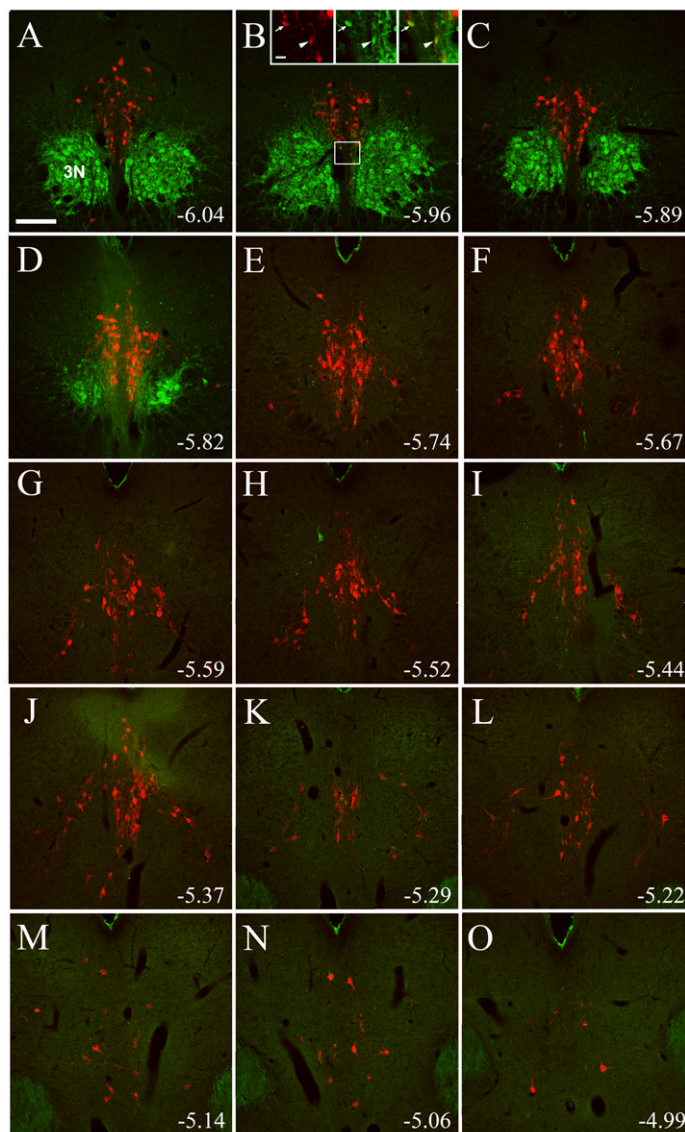


**Figure 1.** Urocortin-1 (Ucn-1)- and choline acetyltransferase (ChAT)- containing neurons within the Edinger-Westphal (EW) nucleus and its vicinity. Ucn-1 was visualized with a red fluorophore, while ChAT was tagged with a green fluorophore. Images were taken from the caudal-most extent of Ucn-1 signal (A) to its most rostral (O). Based on the observed pattern of labeling, we divided the EW nucleus into three anatomical levels: Caudal (A-D), Middle (E-J), and Rostral (K-O). Caudally, Ucn-1-containing neurons form a rhomboid-like shape located dorsomedially relative to the third nerve nucleus (3N), which forms a circular structure made up of ChAT-positive neurons (A-D). We defined the Middle level as the region rostral to 3N where in addition to the column of Ucn-1 neurons along the midline, a second population of Ucn-1-positive cells formed a ventrolaterally displaced diagonal band. With the most rostral portion of the Edinger-Westphal nucleus, Ucn-1 cells are sparse and dispersed. Occasional ChAT/Ucn-1 double-labeled cells were detected (B, inset) with the majority of such neurons located with the Middle level. Numbers refer to approximate distances from bregma in mm. Scale bars: 200  $\mu\text{m}$ ; 20  $\mu\text{m}$  (inset).

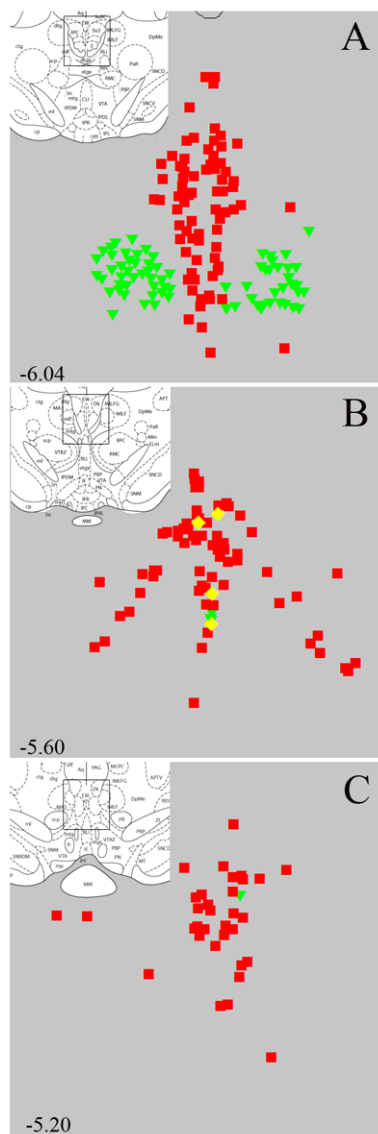


**Figure 2.** Distribution of neurons expressing ChAT and Ucn-1. Images illustrate locations of ChAT (green), Ucn-1 (red), and ChAT/Ucn-1 double-labeled (yellow) neurons mapped from a representative animal. Each symbol represents the location of one neuron on one section from the Caudal (A), Middle (B), and Rostral (C) levels of EWcp as defined in Figure 1. Approximate rostro-caudal location of each section is indicated by distance from Bregma in mm. Corresponding atlas plates from the atlas of Paxinos and Watson (Paxinos and Watson, 1998) are presented in the insets. Note that Ucn-1/ChAT double-labeled cells were found predominantly along the midline at Level 2 (B).

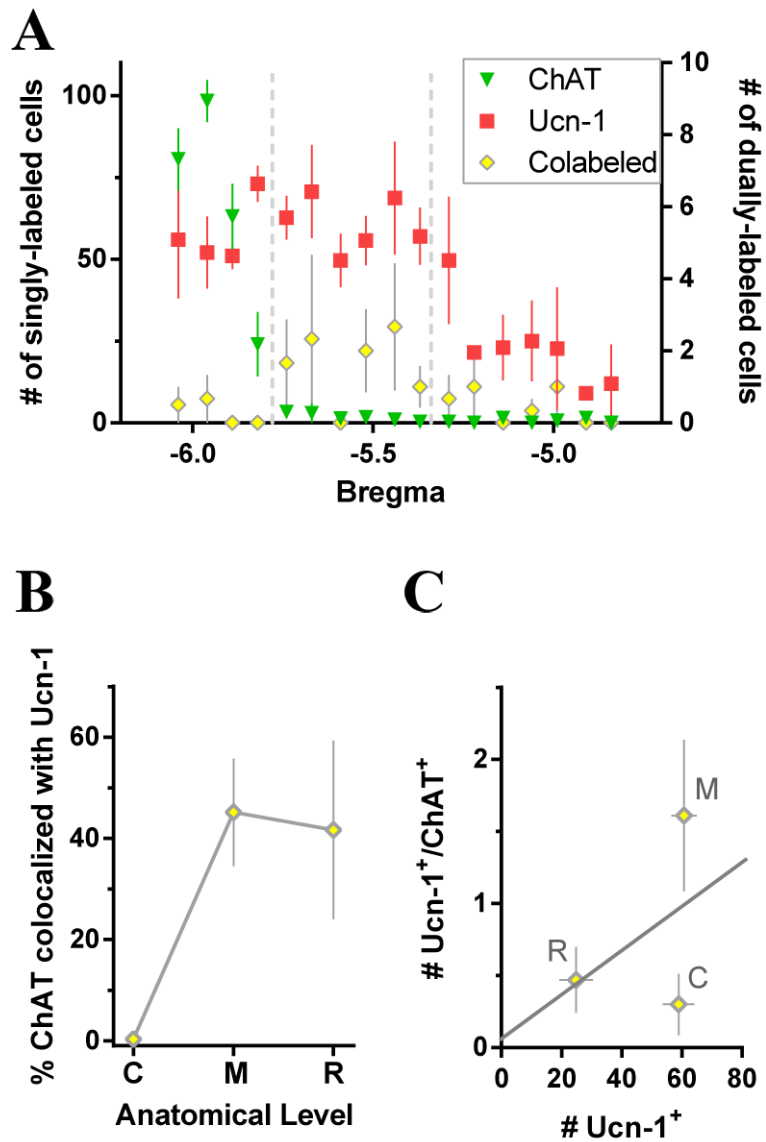


**Figure 3.** Comparison of ChAT and Ucn-1 immunoreactivity across levels. (A) Ucn-1<sup>+</sup> neurons are highest in the caudal and middle regions of the EWcp, while ChAT<sup>+</sup> neurons are highest in the most caudal region. Co-labeled cells are highest in the middle region (right y axis). Dashed lines indicate our demarcations for Caudal, Middle, and Rostral portions of the EWcp. (B) Almost 50% of all ChAT<sup>+</sup> neurons in the Middle (M) and Rostral (R) regions are also Ucn-1<sup>+</sup> positive, while few in the Caudal (C) region are. (C) The number of co-labeled cells is not simply a function of the number of Ucn-1<sup>+</sup> cells, as seen by the differences in between the caudal (C) and middle (M) regions. In all cases, data points represent the mean ± SEM of the appropriate measurement. Statistics are presented in the text and Table 3.

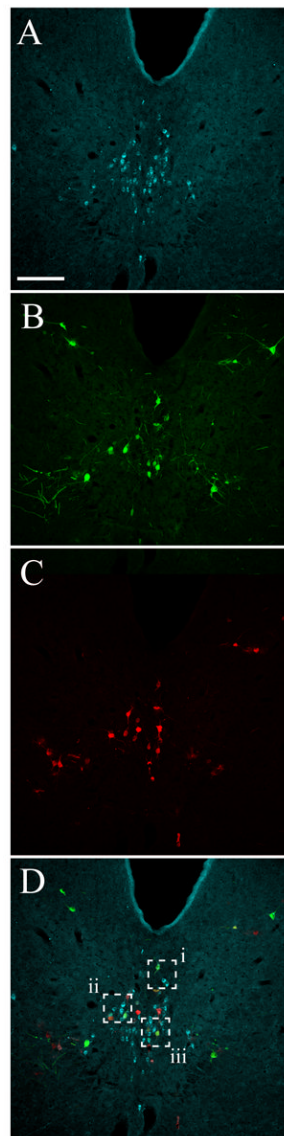


**Figure 4.** Distribution of PRV signal relative to Ucn-1. Images were taken from a representative animal in the intermediate survival group from the Middle rostro-cauda. Ucn-1 (A), PRV-152 (B), PRV-BaBlu (C), and merge of the three signals (D) are illustrated. Areas designated by boxes in D are shown at higher magnification in Fig. 5. Scale bar, 20  $\mu\text{m}$ .

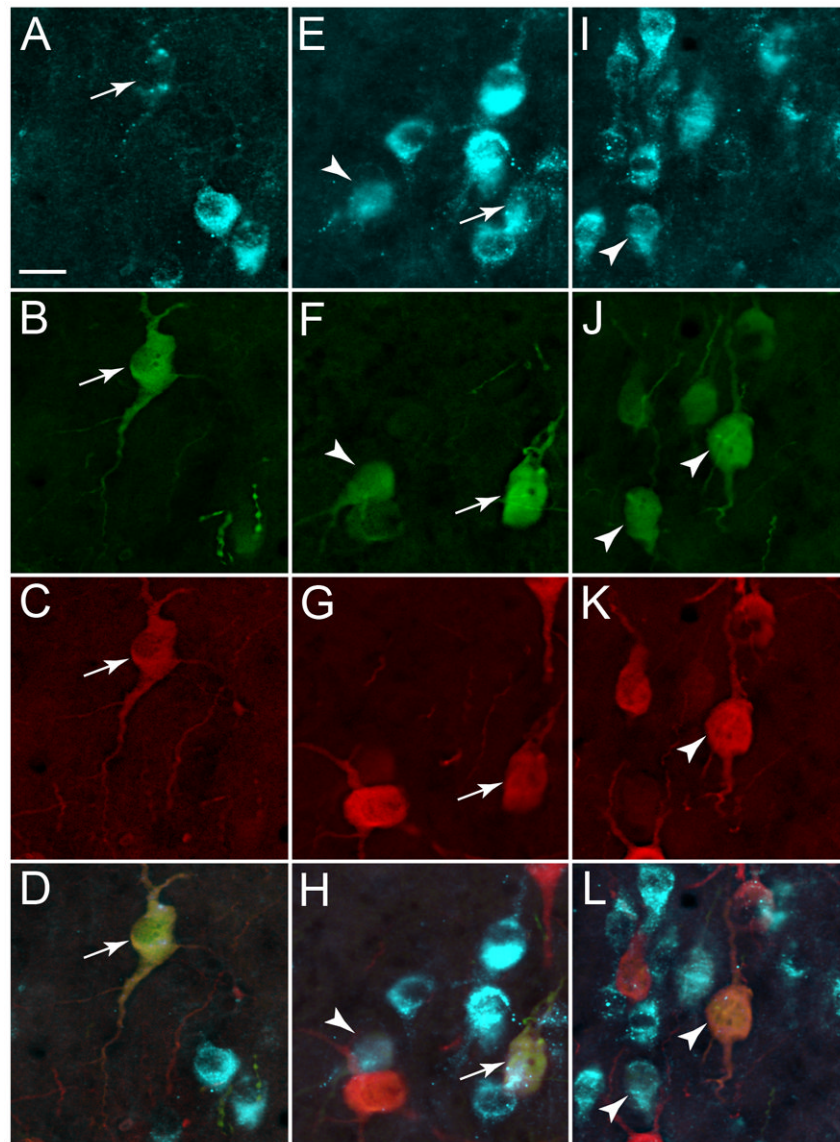


**Figure 5.**

Examples of Ucn-1 co-localization with PRV-152 and PRV-BaBlu. All images were taken from areas shown by boxes in Fig. 4. Box i in Fig.4 corresponds to panels A-D, ii – E-H, and iii – I-L. Images were taken from the same field of view and show labeling for: Ucn-1 (A, E, I), PRV-152 (B, F, J), PRV-BaBlu (C, G, K), and merge (D, H, L). Examples of triple- and double- labeled neurons are shown with arrows and arrowheads, respectively. Scale bar: 200  $\mu$ m.

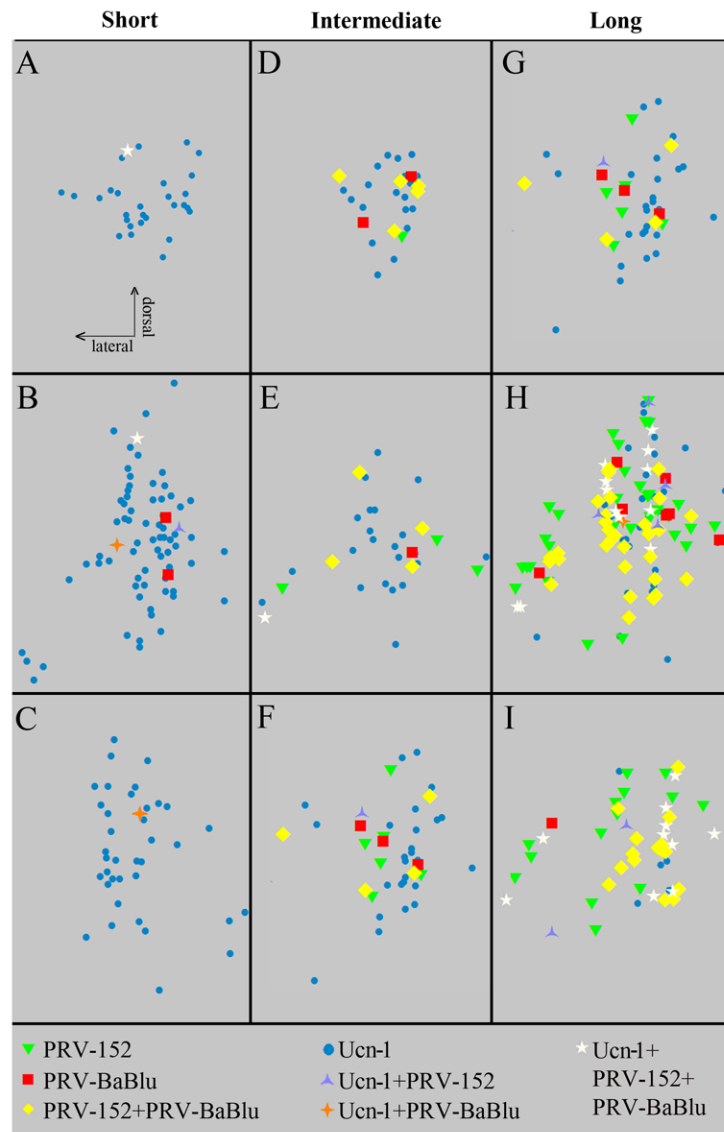


**Figure 6.** Distribution of Ucn-1 and PRV-infected neurons. Maps were generated utilizing NeuroLucida software (MBF Bioscience). Distribution of labeling in a representative animal from the short (A-C), intermediate (D-F), and long (G-I) survival groups are shown. Each symbol shows location of an individual neuron from one section.

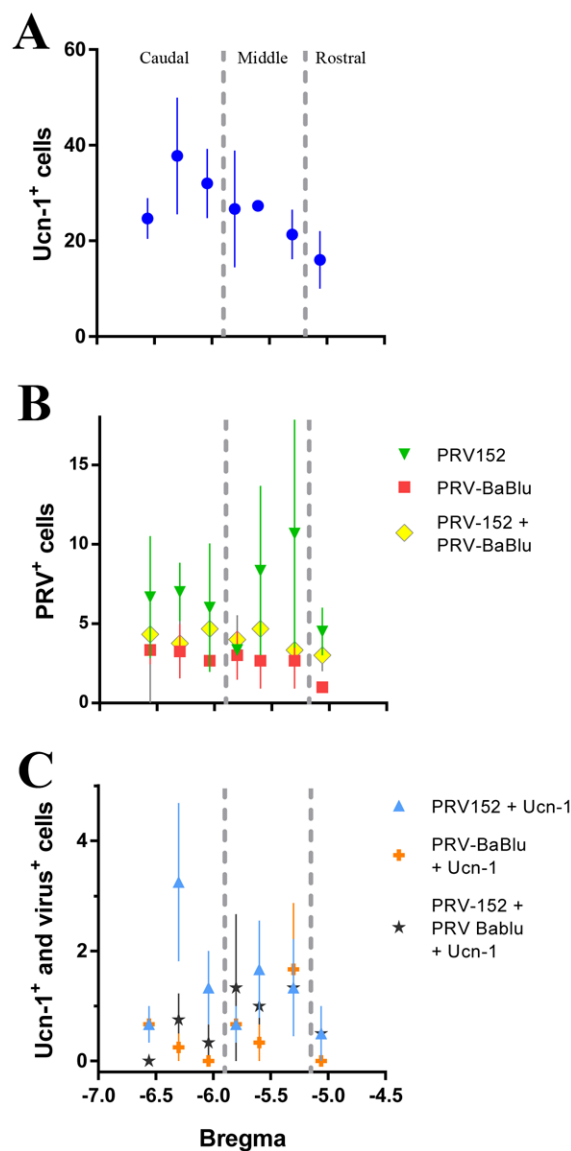


**Figure 7.** Comparison of distributions of neurons in PRV-infected animals. Both the number of Ucn-1<sup>+</sup> (A) and PRV<sup>+</sup> (B) neurons were relatively constant across the rostral-caudal extent of the EWcp. The number of Ucn-1<sup>+</sup>/PRV<sup>+</sup> neurons (C) appeared higher in the caudal and middle portions, but this did not reach statistical significance. Data points represent mean ± SEM at each Bregma level. Only levels with at least 2 sections were included in the graphs. For averages across the subregions of the EWcp, see Table 3.

**Table 1**

## Experimental Groups

Rat ID	Post-Injection Survival Times (hrs.)		Group
	PRV-BaBlu	PRV-152	
1	96	120	Short
2	97	122	
3	108	132	Intermediate
4	108	132	
5	112	136	
6	119	143	
7	111	144	Long
8	120	144	

A total of 8 animals were used in our study, with survival times ranging from 96-120 hrs post PRV-BaBlu and 96-144 hrs post gastrocnemius muscle injections. Rats were grouped into the: Short, Intermediate, and Long survival groups based on their post-injection survival times and infection levels. Rat #6 was assigned to the Intermediate group, because of the pattern of PRV-152 expression within the EWcp.

**Table 2**Ucn-1<sup>+</sup> Neurons within EWcp.

Level	Cell Type	Number/Section	N
Caudal	Ucn-1 <sup>C</sup>	59.2 ± 5.1	10
	Ucn-1 <sup>PRV</sup>	34.8 ± 5.0 <sup>‡</sup>	11
	Ucn-1/ChAT <sup>C</sup>	0.3 ± 0.2	10
Middle	Ucn-1 <sup>C</sup>	62.3 ± 4.1	18
	Ucn-1 <sup>PRV</sup>	29.8 ± 6.3 <sup>‡</sup>	6
	Ucn-1/ChAT <sup>C</sup>	1.6 ± 0.5	18
Rostral	Ucn-1 <sup>C</sup>	30.6 ± 6.3 <sup>*</sup>	19
	Ucn-1 <sup>PRV</sup>	23.5 ± 4.0	6
	Ucn-1/ChAT <sup>C</sup>	0.4 ± 0.2	19

Numbers of Ucn-1<sup>+</sup> neurons were quantified in the brains of rats injected with colchicine (Ucn-1<sup>C</sup>) or with PRV (intermediate survival time, Ucn-1<sup>PRV</sup>). A small number of Ucn-1/ChAT double-labeled neurons was detected in colchicine-treated animals. Data are presented as number of neurons per section (mean ± SEM) at the three rostro-caudal levels of EWcp (see text for more details).

\* p < 0.01 vs. Caudal and Middle levels;

<sup>‡</sup> p < 0.01 vs. Ucn-1<sup>C</sup> at the same neuroanatomical level, N represents the number of sections.

**Table 3**

## PRV-Labeled Neurons within EWcp.

Anatomical Level	Cell Type	Number/Section
Caudal (n = 11)	PRV-152	6.7 ± 1.7
	PRV-BaBlu	2.9 ± 0.6
	PRV-152+PRV-BaBlu	4.0 ± 1.3
	PRV-152+Ucn-1	2.4 ± 0.8
	PRV-BaBlu+Ucn-1	0.3 ± 0.1
	PRV-152+PRV-BaBlu+Ucn-1	0.5 ± 0.2
Middle (n = 9)	PRV-152	7.4 ± 2.8
	PRV-BaBlu	2.8 ± 0.8
	PRV-152+PRV-BaBlu	4.0 ± 0.8
	PRV-152+Ucn-1	1.2 ± 0.4
	PRV-BaBlu+Ucn-1	0.9 ± 0.4
	PRV-152+PRV-BaBlu+Ucn-1	1.2 ± 0.5
Rostral (n = 3)	PRV-152	5.0 ± 1.0
	PRV-BaBlu	1.7 ± 0.7
	PRV-152+PRV-BaBlu	3.3 ± 0.7
	PRV-152+Ucn-1	1.0 ± 0.6
	PRV-BaBlu+Ucn-1	–
	PRV-152+PRV-BaBlu+Ucn-1	0.3 ± 0.3

At the intermediate survival time, numbers of neurons infected with the PRV recombinants were quantified at the three rostro-caudal levels within EWcp. Data are presented as number of neurons per section (mean ± SEM), with *n* being the number of sections used for the quantification.